Manuscript refereed by Dr Stefano Lionetti (RINA Consulting, Italy)

Morphological Evaluation of Metal Powder to Predict Performance in Powder Bed AM

E. Rahimi[1]   ehsan.rahimi@mpiuk.com;   A. Hunt[1]   adam.hunt@mpiuk.com;   X. Hao[2] xinjiang.hao@libertysteelgroup.com

[1]Materials Processing Institute, UK
[2]Liberty Powder Metals, UK

Abstract

Physical properties of metal powder such as flowability, spreadability and packing density are critical to the performance of powder bed additive manufacturing (AM) processes. This research offers a versatile approach to evaluating metal powders for the laser powder bed fusion (L-PBF) process by correlating morphological classifications against the physical properties of the powder and processability during the powder bed re-coating process. Static image analysis was used to measure and classify the powders by a predefined set of rules based on shape descriptors of the powders. These classification groups quantify the powders in terms of highly circular, circular, minor satellited, major satellited, elongated, agglomerated and undersized particles. These classifications were compared against data from a rotating drum test and an automated dynamic tap density analyser. A new weighted index has been proposed to represent the combined influence of size and morphological classifications on the flowability and processability of powders for L-PBF.

Introduction

Flowability of powder is mainly influenced by the particle size distribution and shape, electrostatic charge, moisture content, density and surface properties. Several researchers have studied the individual powder characteristics for the additive manufacturing (AM) re-coating process.[1-4] However, the combined influence of flowability, size and morphological distribution have not yet been assessed. Various methods for the descriptive and quantitative representation of particle shape and morphology have been studied. International standards such as ISO 9276 and ISO 13322 give guidance on the methodologies for the size analysis and morphological descriptors.[5] However, there is no standard quantitative methodology for morphological classifications of metal powders to be used in laser powder bed fusion (L-PBF) process. It is essential to define a simplified parameter to represent the dominating morphological group classifications such as the circularity, alongside the size distribution. The aim of this research, carried out using the dedicated powder laboratory at the Materials Processing Institute, is to introduce an approach to represent the dominating parameters of powder characteristics in the L-PBF process. This approach also includes the inconsistencies in post-atomisation processing of metal powder such as industrial sieving that leads to batch-to-batch variation from undersized carryover.

Methodology

All samples were 316L stainless steel, produced by several suppliers at varying gas atomisation process parameters. These parameters included nozzle design, atomising gas pressure and gas temperature. Table 1 shows the particle size distribution of 316L stainless steel samples used in this study.

Table 1: Particle size distribution of 316L stainless steel samples.

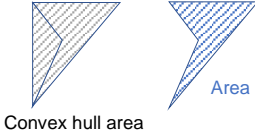| ID	D10	D50	D90	ID	D10	D50	D90
1	23.38	32.39	40.04	**11**	19.41	25.55	35.96
2	22.58	24.43	39.5	**12**	18.76	25.75	36.54
3	20.35	27.78	38.35	**13**	19.33	25.48	38.47
4	19.99	28.48	38.81	**14**	19.63	28.01	38.28
5	20.18	28.88	40.61	**15**	19.83	30.09	42.79
6	19.57	26.62	37.59	**16**	21.66	28.73	49.64
7	17.08	25.94	37.13	**17**	16.62	26.67	37.94
8	21.17	28.83	39.49	**18**	16.46	23.61	37.48

9	20.62	30.64	41.28	19	23.74	30.54	40.13
10	22.34	26.97	37.97	20	22.96	28.65	40.73

Static Image Analysis

The powder size and morphology were evaluated using a Malvern Morphologi 4.0. This instrument is based on an automated optical microscopy system that analyses individual particles with image analysis software. Group classifications were used to quantify morphological type, those groups being highly circular, circular, minor satellited, major satellited, elongated, agglomerated and undersized particles. These classifications were developed empirically and based on the defined boundaries on the measured geometrical descriptors. The size distribution was also reported based on the circular equivalent (CE) diameter of every particle.

A standard operating procedure was developed for the sampling size, dispersion energy and scan area. The powders were dispersed in a dry condition through a sample dispersion unit (SDU). Sample scoop sizes between 1 mm and 7 mm were trialled. The initial measurements showed that a scoop size with a 1 mm diameter and a low dispersion pressure of 1 bar resulted in the fewest agglomerates and therefore gave a more consistent orientation of the 316L particles on the glass plate. The dispersion injection time was set to 20 ms, and the settling time was raised to 60 s. To ensure clarity and consistency of the images, a 10X magnification lens was used and the focus was applied manually for every analysis. Three samples were analysed from each batch and the average results were reported for each classification. Morphology classifications were defined by boundaries on specific morphological descriptors. Table 2 illustrates the morphological descriptors and their formula used in this research.
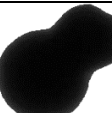
Table 2: Morphological Descriptors[6]

Descriptor	Definition
HS Circularity	Degree to which a particle is similar to a circle, considering the smoothness of the perimeter. $$HS\ circularity = \frac{4\pi \times Area}{perimeter}$$
Convexity	$$Convexity = \frac{Convexity\ hull\ perimeter}{perimeter}$$ Convexity hull perimeter is the perimeter of the convex hull bounding the particle.
Solidity	Measure of the overall concavity of the particle. $$Solidity = \frac{Area}{Convex\ hull\ area}$$ Convex hull area is the area of the convex hull bounding the particle.
Elongation	For very elongated particles: $$Elongation = 1 - \frac{width}{length}$$
CE Diameter	Circle equivalent diameter

Defined boundaries were developed and applied on one, or a combination of shape descriptors to quantify each classification group. The definitions were based on the observation of individual particles and they were experimentally examined for all samples. Table 3 displays the definitions and an example for each classification. In addition to the morphological classification, an undersized classification was also determined to quantify the powders with CE diameter smaller than 15 µm that is out of the typical L-PBF size range (15-45 µm). All morphological classifications and size distributions were quantified by volume. There is no global standard for morphological classification of metal powders for AM. Therefore, to find a correlation between the size and classification group and the parameters of compaction and flowability, a general circularity classification that covers both highly circular and circular particles is

proposed. This classification group includes every particle with HS Circularity higher than 0.96. (1 being a perfectly circular). This classification is called the circularity ratio (the sum of highly circular and circular particles in Table 3).

Table 3: Developed Morphology Classifications

Classification	Definition	Example
Highly Circular	*0.98≤HS Circularity*	
Circular	*0.96≤HS Circularity<0.98*	
Minor Satellites	*0.75≤HS Circularity<0.96* *0.95<Convexity* *0.965<Solidity* *10>CE Diameter* *Elongation<0.45*	
Major Satellites	*0.75≤HS Circularity<0.96* *0.95<Convexity* *Solidity≤0.965* *CE Diameter>10*	
Agglomerates	*Solidity<0.94*	
Elongated	*0.45<Elongation* *0.95<Solidity*	

Flowability and Compaction

The flowing angle and cohesive index (CI) were measured in a dynamic condition with an automated rotating drum instrument, the GranuDrum. The unit cell was half filled with the powder sample (55 ml, approximately 240 g). The drum rotated around its central axis at a speed of 1, 5, 10, 20 and 30 rpm in both increasing and reverse orders. A Charged-Coupled Device (CCD) camera took 60 images for each angular velocity. The image sampling was set at 1000 ms. The air/powder interface was detected on each captured image with a thresholding edge detection algorithm. For each rotating speed the dynamic angle of repose (flowing angle) was computed from the average interface angle and the dynamic CI was computed from the fluctuations around this average interface position. In general, a low value of flowing angle leads to a good flowability. A dynamic cohesive flow closing to zero corresponds to a non-cohesive powder.[6] The samples were examined twice and the average results were reported. The correlation of the flowability and morphology were plotted based on a rotating speed of 10 rpm in increasing order.

The dynamic evolution of the bulk and tap density was measured by an automated dynamic tap density instrument, the GranuPack. For the test 35 ml of powder (approximately 160 g) was used for each sample and the tap density parameters including initial density, final density, Hausner ratio (Hr), and n½ (number of taps to reach half the final compaction) were measured. The density measurements as a function of the tap number show the evolution and kinetic properties of the powder.[7] The results are the average of two measurements on each sample. A total of 1200 taps were completed for each measurement. Further taps were seen to give errors due to powder escaping around a diabolo placed on the surface of the powder to allow a sensor to measure the powder height.

Laser Powder Bed Fusion Process

To verify the powder flowability in the AM re-coating process, the cylindrical tensile blanks were made in the Concept Laser Mlab200R for selected samples. The re-coater speed for spreading the powder was set between 50 to 75 mm/s. According to previous research on optimisation of the re-coater speed, this speed is equivalent to 10-20 rpm in the GranuDrum instrument. The reported optimum re-coater speed (40 rpm) was high for a small build plate used in this research, and at such speeds, all samples were seen to have similar spreadability at this speed in the re-coater process. Since the flowing angle

showed an increasing trend for most samples, a moderate re-coater speed was chosen for a better comparison.[6]

Results and Discussion

Figure 1 displays the morphological distribution based on the defined group classifications. The amount of undersized particles are represented separately as it is distinct from the morphology classifications. The circularity ratio is in the range of 50-60% for most samples. Samples 1, 2, 5, 19, 20 had a circularity ratio below the average level (54.55%). Sample 5 contained the most total satellites (42.6%) and sample 17 had the fewest total satellites (29.32%). Sample 5 had an unusual distribution with the lowest circularity ratio (37.7%) and the highest agglomerates (20%) which is attributed to the gas atomisation parameters. The three main morphological and size classifications (total circular, total satellited and undersized) were used to evaluate the influence of morphology on powder flowability in this research.
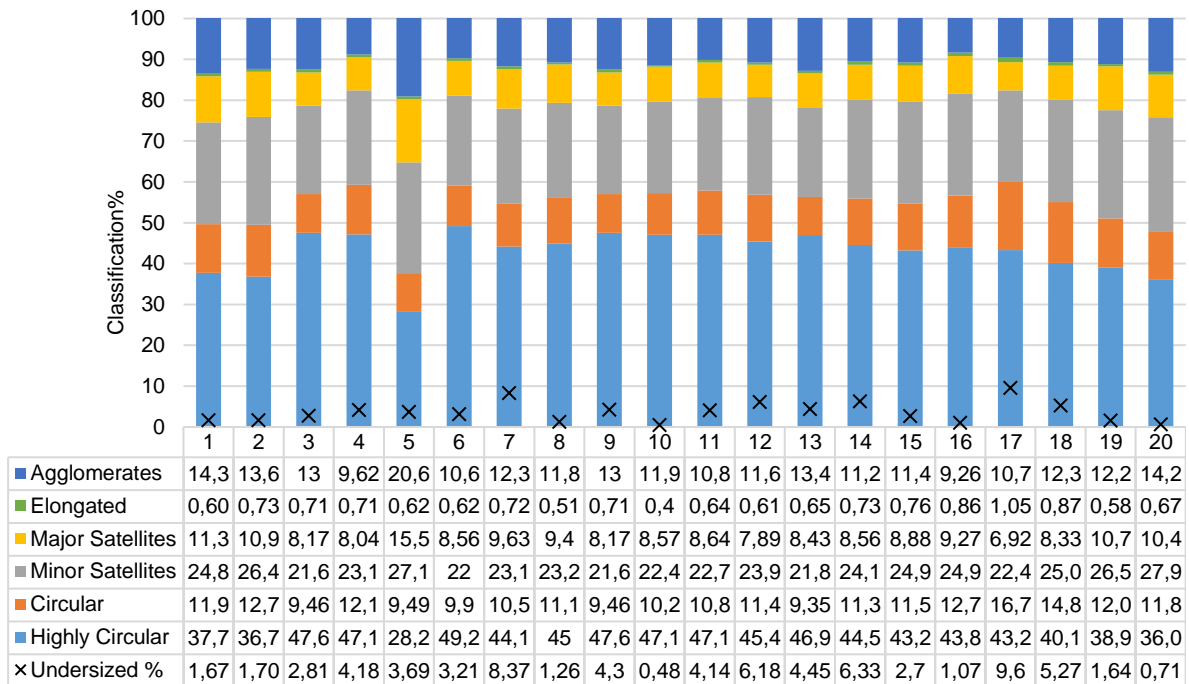
	1	2	3	4	5	6	7	8	9	10	11	12	13	14	15	16	17	18	19	20
■ Agglomerates	14,3	13,6	13	9,62	20,6	10,6	12,3	11,8	13	11,9	10,8	11,6	13,4	11,2	11,4	9,26	10,7	12,3	12,2	14,2
■ Elongated	0,60	0,73	0,71	0,71	0,62	0,62	0,72	0,51	0,71	0,4	0,64	0,61	0,65	0,73	0,76	0,86	1,05	0,87	0,58	0,67
■ Major Satellites	11,3	10,9	8,17	8,04	15,5	8,56	9,63	9,4	8,17	8,57	8,64	7,89	8,43	8,56	8,88	9,27	6,92	8,33	10,7	10,4
■ Minor Satellites	24,8	26,4	21,6	23,1	27,1	22	23,1	23,2	21,6	22,4	22,7	23,9	21,8	24,1	24,9	24,9	22,4	25,0	26,5	27,9
■ Circular	11,9	12,7	9,46	12,1	9,49	9,9	10,5	11,1	9,46	10,2	10,8	11,4	9,35	11,3	11,5	12,7	16,7	14,8	12,0	11,8
■ Highly Circular	37,7	36,7	47,6	47,1	28,2	49,2	44,1	45	47,6	47,1	47,1	45,4	46,9	44,5	43,2	43,8	43,2	40,1	38,9	36,0
✕ Undersized %	1,67	1,70	2,81	4,18	3,69	3,21	8,37	1,26	4,3	0,48	4,14	6,18	4,45	6,33	2,7	1,07	9,6	5,27	1,64	0,71

Figure 1. Morphological and size classifications.

Figures 2 and 3 show the CI and flowing angle respectively for each sample at various speeds. No hysteresis was observed during the decreasing order, so only the increasing order is reported. Sample 1 shows the highest CI (above 35 at all speeds). This sample has a low circularity, moderate satellites, and high agglomerates (14.38%). The cut-off values for CI and flowing angle are 25 and 37° respectively, below which successful L-PBF processing is assumed.[8]
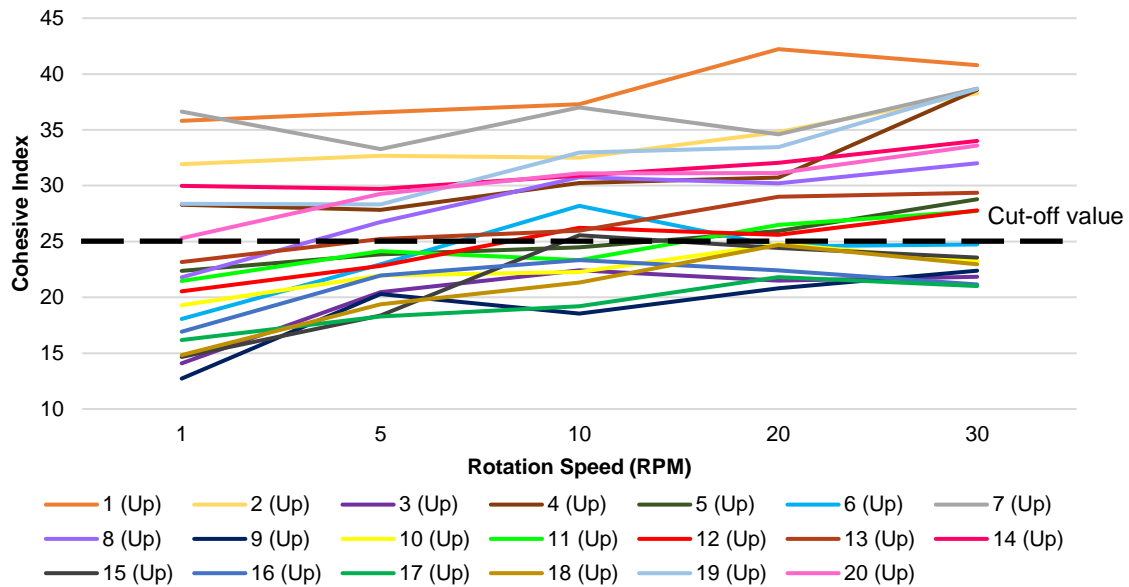
Figure 2. Cohesive index versus rotating speed. The cut-off value is 25. (UP=increasing speed)
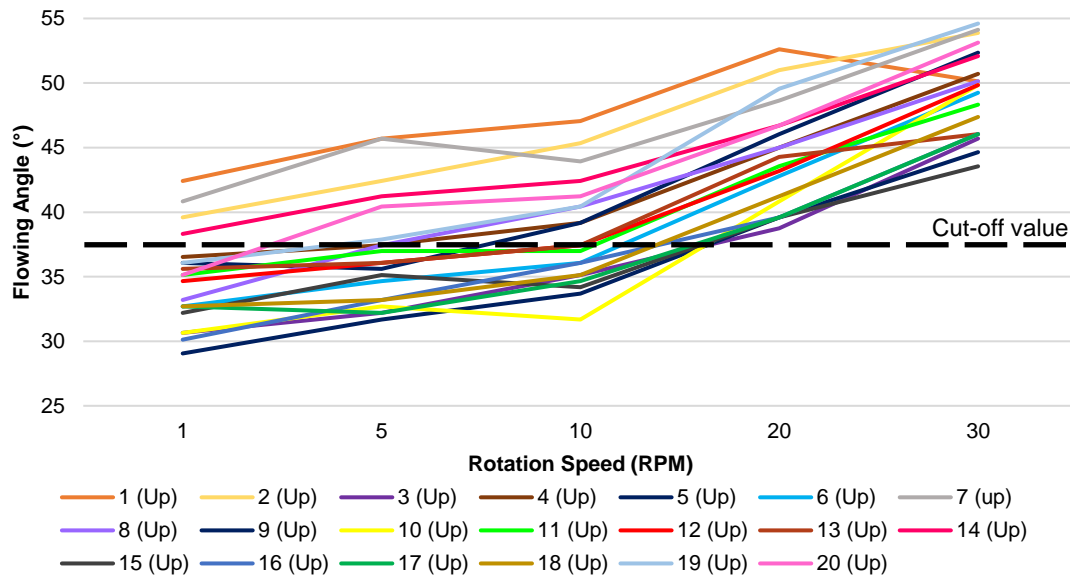

Figure 3. Flowing angle versus rotating speed. The cut-off value is 37°. (UP=increasing speed)

The results in Figures 2 and 3 show that the metal powder has a non-Newtonian rheological behaviour. At increasing rotation speeds, equating to higher re-coater speeds, the CI and flowing angle increases. At higher rotation speeds (20 and 30 rpm), there are still some powders below the cut-off value for CI. Conversely, for flowing angle, none of the powders are below the cut-off value at higher rotation speeds. From these tests, flowability is seen to be more sensitive to change in shear rate compared to CI.

Figures 4 and 5 show the CI and flowing angle, respectively, at 10 rpm (increasing order) versus Hausner ratio. There is a strong positive correlation seen in both Figure 4 and 5. Assuming that the upper limits for the CI and flowing angle are 25 and 37° respectively, a sample with Hausner ratio smaller than 1.17 had a good flowability. Using these values, the L-PBF zone for each plot was estimated. This zone includes all the samples with the ideal flowability and spreadability in the L-PBF process, based on the pre-determined values.
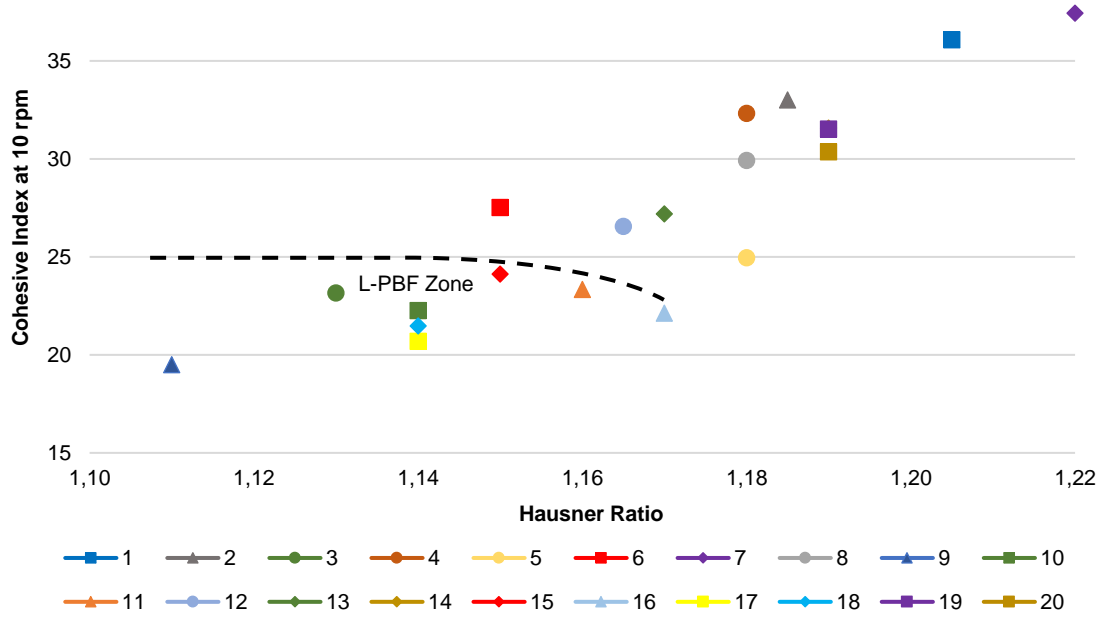
Figure 4. Cohesive index at 10 rpm versus Hausner ratio and the L-PBF limit.
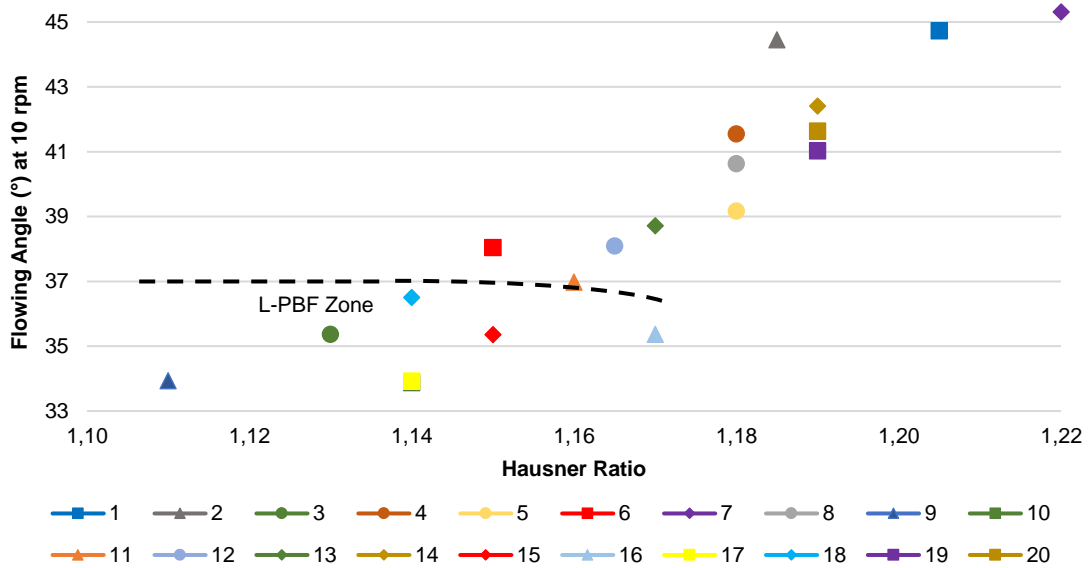

Figure 5. Flowing angle at 10 rpm versus Hausner ratio and the L-PBF limit.

To investigate the correlation with morphological distribution, the CI and Hausner ratio were plotted against the total amount of circular particles (Figures 6 and 7). The correlation in each of these plots is poor, suggesting other parameters contribute to powder flowability and spreadability. The L-PBF zone in these plots includes all the samples with a circularity above 55% and CI and Hausner ratio smaller than 25 and 1.17 respectively.

Samples 3, 9, 10, 11, 15, 17, 18 showed an excellent spreadability in the re-coating process. The spreadability of sample 16 was acceptable and is seen to be on the limit of the L-PBF zone in Figure 6. Sample 6 was out of the L-PBF zone in Figure 7. However, this sample still showed an acceptable spreadability in the re-coating process. The other out-of-zone samples were also processable during L-PBF trials; however, the consistency of the powder layers, especially in the early stages of the build were poor. The poor performing powders may require modified build parameters to improve final part quality.
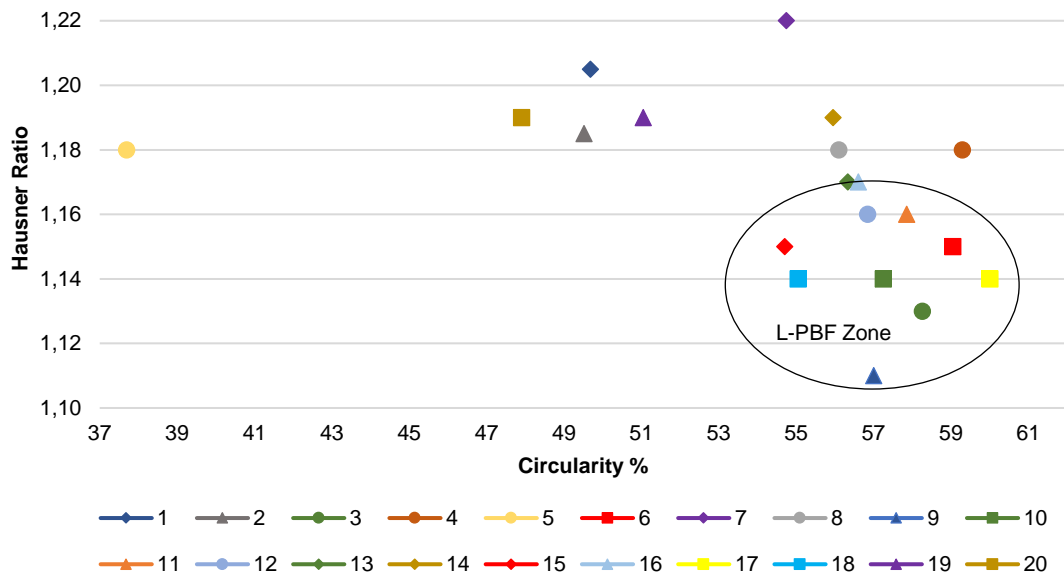
Figure 6. Hausner ratio vs circularity content.
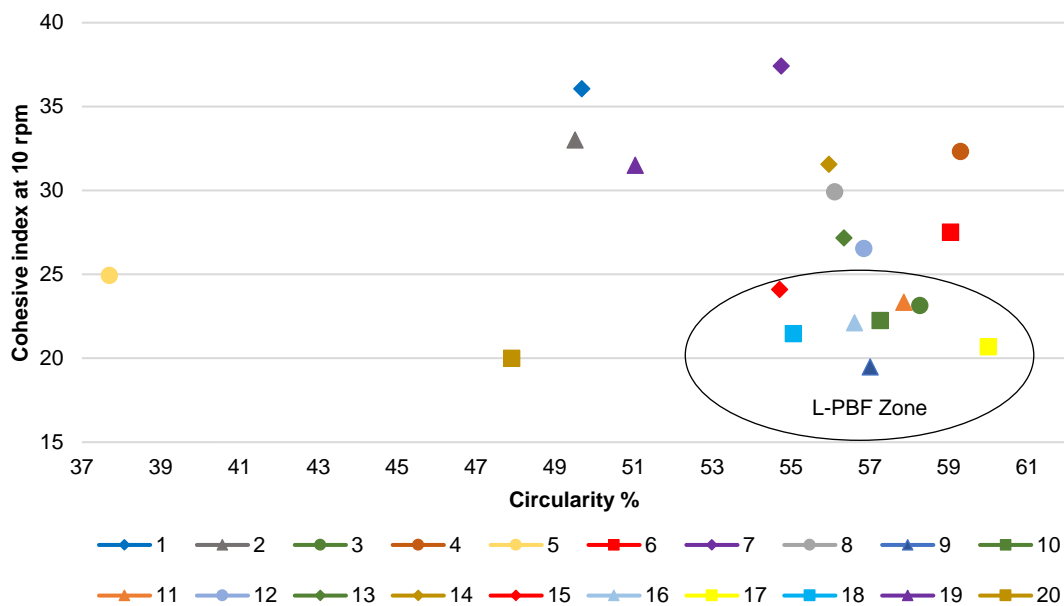

Figure 7. Cohesive index at 10 rpm vs circularity content.

Due to the poor correlation in Figures 6 and 7, a new index is proposed to represent the combined effect of morphology and undersized fraction on flowability. The index is represented in Equation 1 below:

$$Flowability\ index = \frac{a}{C - bS - cU} \qquad \textbf{Equation 1}$$

Where a, b, and c are unitless coefficients, C is the percentage of circular and highly circular particles, S is the percentage of minor and major satellites and U is the percentage of undersized particles by volume. This flowability index was developed so that an index below 1 indicated acceptable flowability for re-coating processes and an index above 1 indicated unacceptable flowability for re-coating processes. To develop the flowability index, the index was correlated against the measured flowing angle at 10 rpm for the powders investigated. Sample 5 was ignored as an outlier. Using linear regression analysis, the values for coefficients b and c that gave the strongest correlation were 1.06 and 1.69 respectively. The value for coefficient a was adjusted to 17 so that a flowability index of 1 predicted a flowing angle of 37°, the threshold for acceptable powder. The plot of flowability index against flowing angle can be seen in Figure 8.
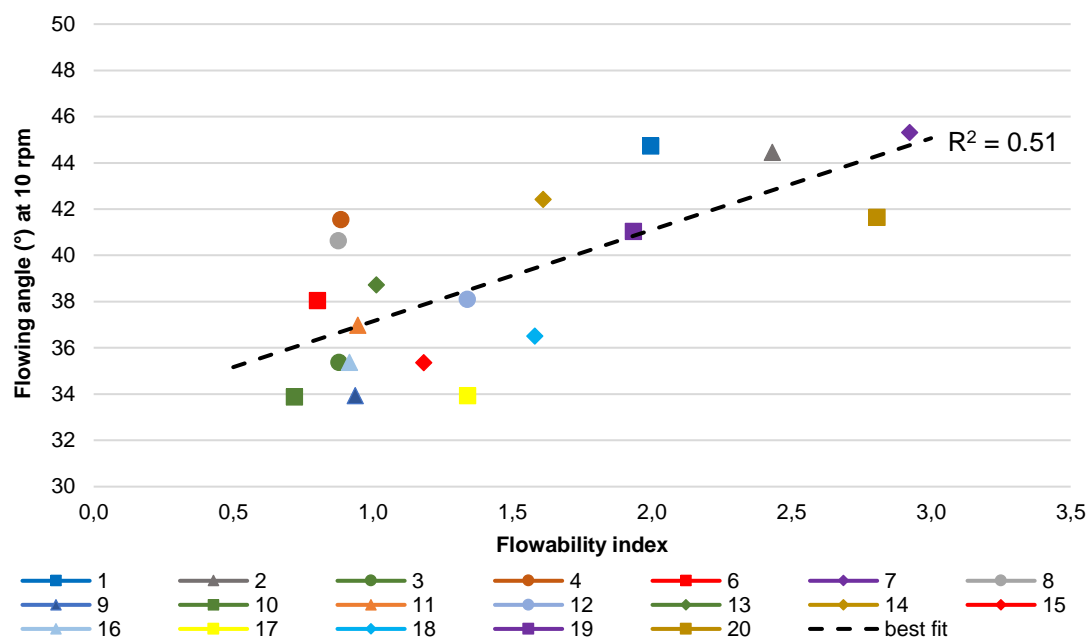
Figure 8. Newly proposed flowability index vs flowing angle at 10 rpm.

In general, there is good agreement between the new flowability index and flowability measurement, especially at higher flowing angle. Most of the powders identified as being in the L-PBF zone (Figures 4 to 7) had a flowability index below 1. From experience, powders with a flowability index between 1 and 2 may still be able to be used in the L-PBF process, but printing parameters may need to be adjusted to give suitable quality in the final part.

This index does not include the surface roughness of the powder, the influence of sub-grains surrounding the particles, the moisture content, and the variation in flowability due to irregular morphologies, e.g., the different influences of elongated and agglomerated particles. The variability in these parameters is a likely cause of the reduced correlation coefficient in Figure 8. Further work is planned to account for these parameters and improve the newly proposed flowability index.

Conclusions

- Static image analysis has been used to develop a method for classifying gas atomised metal powder in terms of morphology groups.
- In the absence of a global standard for morphological distribution for the AM powders, circularity above 0.96 can be used as the main morphological classification. An undersized classification can be used to define batch-to-batch variations in sieving and operations.
- A very strong correlation was seen between the physical properties of cohesive index, flowing angle, and Hausner ratio.
- A new index has been proposed to determine the suitability of a powder for the re-coater process based on morphology and size alone. In most cases this index was seen to be in good agreement with the observations during AM.

Acknowledgements

References

1. R. Baitimerov, P. L. (11 (2018)). Influence of powder characteristics on processability of AlSi12 alloy fabricated by Selective Laser Melting. *Materials*, 742. https://doi.org/10.3390/ma11050742.

2. Mussatto, R. G.-H. (182 (2019)). Evaluation via powder metallurgy of nano-reinforced iron powders developed for selective laser melting applications. *Materials & Design*, 108046. https://doi.org/10.1016/j.matdes.2019.108046.

3. Pleass, S. J. (24 (2018)). Influence of powder characteristics and additive manufacturing process parameters on the microstructure and mechanical behaviour of Inconel 625 fabricated by Selective Laser Melting. *Additive Manufacturing*, 419-431. https://doi.org/10.1016/j.addma.2018.09.023.

4. S.E. Brika, M. L. (31 (2020)). Influence of particle morphology and size distribution on the powder flowability and laser powder bed fusion manufacturability of Ti-6Al-4V alloy. *Additive Manufacturing*, 100929. https://doi.org/10.1016/j.addma.2019.100929.

5. ISO 9276-6. (2008). ISO9276-6. In *Representation of results of particle size analysis; Part 6: Descriptive and quantitative representation of particle shape morphology.* International Organization for Standardization.

6. Granutools. (2020, Aug 5). *Understanding and improving powders spreadability for a recoater process in Additive Manufacturing*. Retrieved from Granutools: www.granutools.com

7. *Granupack operators guide.* (n.d.). Granutools. Retrieved from Granutools: https://www.granutools.com

8. G. Yablokova, M. S.-P. (2015). Rheological behaviour of B-Ti and NiTi powders produced by atomization for SLM production of open porous orthopedic implants. *Powder Technology 283*, 199-209. https://doi.org/10.1016/j.powtec.2015.05.015.